International Journal of Railway Technology
Volume 6 Issue 1, Pages 41-67, 2017.
doi:10.4203/ijrt.6.1.3

SAXE-COBURG
PUBLICATIONS

Onboard Load Sensor for Use in Freight Railcar Applications

C. Tarawneh[1], J. Ley[1], D. Blackwell[1], S. Crown[1], and B. Wilson[2]

[1]University Transportation Center for Railway Safety
University of Texas Rio Grande Valley, Edinburg, Texas
United States of America
[2]Amsted Rail Company, Granite City, Illinois
United States of America

Abstract

Approximately 40% of intercity freight transportation occurs by rail, making it the most widely used method of transporting large commodities. This trend is expected to persist over the next thirty years as our highway systems are strained and experiencing increased congestion and costly delays. Currently, the load of freight railcars is typically measured by weighbridges or retrofitted tracks at isolated locations. This practice is not efficient and limited by the fact that the load of the railcar cannot be monitored continuously, not to mention the inherent inaccuracies of such systems. Hence, there is great merit for an onboard load sensor that can accurately and effectively track the load of a railcar, minimizing overloading issues that can result in costly fines and damages to the rail infrastructure. The proposed onboard load sensor equipped with temperature sensing capability can also be used in bearing condition monitoring, as it will be able to identify unbalanced loading of the railcar. This paper provides proof of concept validation for an onboard railcar load sensor and presents analysis on the accuracy of two proposed correlations: one second-order model, and one multivariate model that incorporates the bearing operating temperature as read by the onboard sensor. The proposed load sensor can be readily implemented in freight railcars with minimal adjustments to the current bearing-adapter assembly. Laboratory testing is used to extrapolate different hypothetical operation scenarios that serve to demonstrate the use of this sensor in field service. The incorporation of the temperature sensors to the proposed onboard load sensing system provides added condition monitoring capability and allows for a much-improved load measurement with an accuracy of within 2% of the actual value.

Keywords: onboard load sensor; freight railcar load measurement; real-time load sensing; railroad bearing load; railcar condition monitoring; multivariate calibration.

1 Introduction

Accounting for weight and distance, rail is currently the most prominent method of intercity freight transportation, leading transportation by truck by 10.9% in 2010. It is described as arguably “the safest, most efficient, and cost effective” method in the world by the Federal Railroad Administration [1]. Yet despite its advantage in efficiency, limitations arise from the fact that all systems of the railcar must work in unison to ensure the safety of the cargo as well as pedestrians. These limitations can end up being the cause of massive, costly derailments. Rail corporations need to oversee the industry to prevent major catastrophes, like the West Virginia incident of 2015, where 26 tanker cars derailed and threatened the water supply of the nearby population [2].

Excessive speeding on curves, track defects, and railcar suspension failures involving events such as hunting or the overheating of defective bearings are the major causes of wheel misalignment, the foremost factor of derailments [3]. Much of railroad research and development focuses on preventative measures targeting the dynamic and static health of each component that lies within the railcar suspension system. One of the most examined components, the double-tapered roller bearing, seen in Figure 1, is a railroad-industry standard because of its durability in response to both axial and radial loads [4]. Currently, there are non-contact devices and techniques employed in the field that aim to monitor the health of bearings, but studies have found these to be somewhat ineffective in identifying the onset of bearing failure [5-6].

Double-tapered roller bearings have several unique mechanical design aspects. The two ends of each roller have different diameters, resulting in a large area of contact, which gives the component the capability to withstand large axial and radial loads. The “cone” or “inner ring” houses the inner raceways in which the rollers operate. While the “cup” or the “outer ring” contains the outer raceway for the rollers and encompasses the entire assembly, as seen in Figure 1. The cage separates the rollers at a fixed distance from each other, ensuring smooth operation and even load distribution. Flange features present on the inner ring actively prevent the roller-cage assembly from leaving the bearing raceways at high speeds [8].

There is presently a high demand for an onboard railcar load monitoring system. Taking inspiration from products presently in use, the aim of this technology is to contain a wireless unit recording and reporting the sensor outputs to a localized computer onboard the railcar, which can then proceed to run the necessary algorithms and provide maintenance data to the operator. This would ensure that if a bearing health issue arises, there is a suitable amount of time to take proactive preventative action. While the prototype version of the product presented in this paper is a hard-wired system, the University Transportation Center for Railway Safety (UTCRS) research group is currently working on finalizing a battery-powered wireless prototype version of the system, which will be the topic of a future publication. Note that the sensors used in this system are low-power sensors with minimal power consumption (< 20 mW).

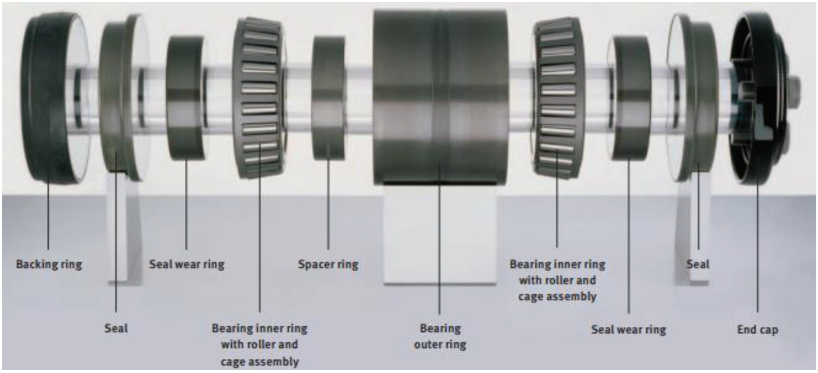

Figure 1: Components of a double-tapered roller bearing [7]

To reach the full potential of this technology, all bearings on the railcar must be equipped with a Smart Adapter™ to completely monitor the load observed by each bearing and produce an immediate response for load imbalances during travel periods. The sensor would inform the operator of any cargo lost or leaks present during travel, which is crucial in the transportation of hazardous liquid freight. In most cases, these hazardous materials have the potential to result in costly damages to urban areas and the environment. Thus, the proposed technology can greatly benefit the railroad industry, and can also help improve and enhance the safety protocols set by the Association of American Railroads (AAR) and the Federal Railroad Administration (FRA).

This paper focuses on the implementation of a load-sensing insert embedded within a Smart Adapter™ that incorporates both a second-order model and a multivariate regression model to compare the measured output of the sensor with the actual load applied to the bearing during operation. The accuracy and efficacy of the final calibrated algorithm is verified through a series of constant load and load ramping scenarios at varying loading rates performed at the UTCRS testing facilities. Moreover, the wired version of the load-sensor prototype system was tested in rail service at the Transportation Technology Center Inc. in Pueblo, Colorado, USA, to verify and validate the reliability and accuracy of the system. The developed load sensor-insert presented here also incorporates two temperature sensors that have the capability to capture the operating temperature of the inboard and outboard raceways of the bearing, allowing for temperature to factor into the load calculation. Hence, this load sensor-insert incorporates two bearing health-assessment measures, providing for a reliable, onboard freight railcar load and temperature condition monitoring system that can be readily implemented with minor modifications to the current bearing-adapter assembly.

2 Technology Review

In the rail industry, bearing-health monitoring systems are expected to detect overworked suspension elements. Studies have shown that temperature, vibration, and load conditions provide most of a bearing's diagnostic information. However, despite this knowledge, the currently utilized method of data collection relies heavily on various types of wayside detectors. These non-contact devices are set along the side of the track; and depending on the type of detector, can measure acoustic or infrared emission properties of the bearings that pass by the system. The Federal Railroad Administration (FRA) has claimed that wayside detectors enhance and supplement existing manual inspection procedures to facilitate early detection of rail defects [9].

The infrared wayside detectors, termed "Hot-Box Detectors," seen in Figure 2, flag a bearing if the temperature becomes greater than 94.4°C (170°F) above the ambient temperature. Most systems typically relate temperature histories as a direct indication of bearing health. Although this method does not determine the root-cause of the problem [10-11], it does provide a warning to indicate necessary bearing inspection or removal. These devices employ two-infrared "eyes" that sit on each side of the track positioned so that the train's bearings will pass above them [12]. Systems that are more current identify bearings that have an operating temperature above the general thermal range of the group in a railcar or train. Once flagged as a "trending" bearing, the removal of the entire axle assembly occurs. This process requires the train conductors to pull over and have workers manually remove the axle in question, which is then sent for a complete disassembly and examination to determine the cause of the bearing temperature increase. Hot-Box Detectors (HBDs) currently lie in 24 to 48 km (15 to 30 mile) increments, placing a limitation on the quantity and quality of temperature data received for each railcar [13].

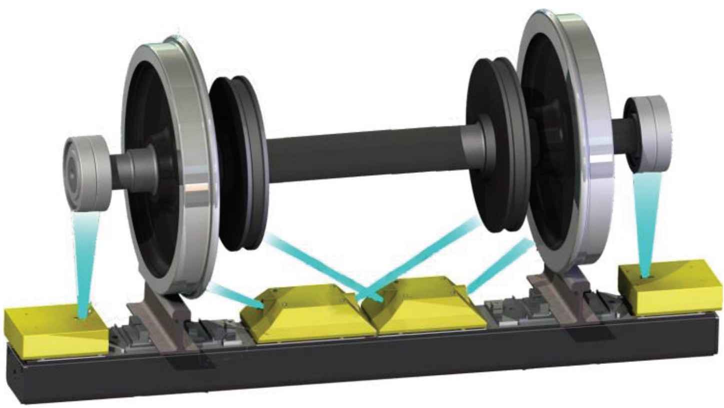

Figure 2: Depiction of a hot-box detector (HBD) [9]

During operation, however, even a relatively healthy bearing can experience fluctuations in operating temperature. These fluctuations, even when exhibiting temperature-trending behavior, are not entirely indicative of a bearing in distress or that of one approaching catastrophic failure. Most currently utilized wayside monitoring systems are not capable of providing accurate predictions of a bearing's remaining service life due to their inability to control factors such as device setup, targeted temperature measurement area, bearing cup discoloration affecting emissivity, and weather conditions. According to data collected by Amsted Rail from 2001 to 2007, an average of nearly 40% of bearing removals are *non-verified*. A non-verified bearing is one that, upon disassembly and inspection, is found not to exhibit any of the commonly documented causes of bearing failure such as spalling, water contamination, loose bearings, broken components, insufficient lubrication, damaged seals, etc." [14]. A more reliable and efficient monitoring system would prevent the costly delays resulting from unnecessary train stoppages and premature removal of healthy bearings. Due to its shortcomings, the current method of wayside detection fails to precisely identify the onset of bearing failure and accurately predict the targeted bearings' health. With freight volumes expected to increase over the next three decades, the benefit of a more dependable bearing-condition monitor system would mean a safer railway system across the board.

Load-sensing wayside detector research is limited. In 2005, Nenov *et al.* [15] published works regarding a procedure used to measure the load experienced by the wheels of a moving railcar. A pair of strain gauges were affixed along the rail in the direction of travel. An algorithm averaging the two strain gauges processed the data acquired and correlated values to an estimated load. Problems arose during the analog-to-digital conversion of the signals, which were later resolved by utilizing a compensating value allowing the linear relationship of the signals to remain intact. Despite the initial promising results, implementation of the technique as a complete health-monitoring device was impractical. Setting the devices in short mileage intervals was an inefficient and laborious practice.

The current methods of load measurement typically involve the use of weighbridges. While railcars drive through a "rail-yard" or a specified section of track, companies will use computerized systems to determine the car weight via large capacity load cells. Most weighbridges stipulate that the car either stop or travel at extremely low speeds, approximately ten kilometers per hour (six miles per hour) [16]. In many cases, for the most accurate measurement, the cars will be uncoupled and weighed separately [17]. Therefore, not only are the rail companies charged for this service, but a large portion of profit is lost in travel time. A database stores the load information received from the weighbridge. If the train is overloaded, the company pays a fine to ensure that future railcars will transport the appropriate weight, providing safety to the track, suspension elements, and wheels [18]. Unfortunately, weighbridges are even less frequent than hot-box detectors (HBDs), which limits their impact on the industry.

The limitations of currently employed detectors have led to the development of what have been termed "smart products." These devices continuously monitor various condition parameters of a railcar system. One of the first milestones in the development of onboard monitoring occurred prior to the implementation of wayside detectors. The instrument, titled the SmartBolt™ consisted of a thermal sensor/actuator connected to a piston and power supply in the form of an endcap bolt [19]. Initially proposed in 1990, the device actively monitored the internal temperatures of the bearing component with the least heat resistance – the seal. Once the seal temperature reached 121°C (~250°F), a signal would be transmitted to the train operator. Despite its potential, this product had a significant drawback. The mechanism lacked the ability to detect temperature spikes. Moreover, outside of a physical inspection, there was no means of resetting the device once it reached the threshold temperature. Consequently, significant time delays and costly product replacements accompanied the integration of this product into rail systems.

An alternative to the SmartBolt™ is the onboard Wireless Sensor Node (WSN). The WSNs have the capability to continuously monitor temperature and send data to a localized computer onboard the railcar, termed the Central Monitoring Unit (CMU). The CMU can then transmit analyses wirelessly by satellite or cellular network and inform the conductor to take preventative actions to avoid any possible derailment or safety issues [20].

The latest smart product in the market is the Timken Guardian Bearing™. An ideal tool for condition monitoring and preventative maintenance, this rolling element can measure the temperature and vibration of the bearing assembly. The sensors have the resolution necessary to diagnose wheel and bearing failure, along with stuck hand brakes, which are a major factor in the overheating of railcar rolling elements [21]. The Guardian Bearing is self-powered and has an internal microprocessor and radio transmitter that can decipher the received data and transmit the results wirelessly. However, the main drawback of this design is the significant capital investment. Moreover, when the system detects a potential problem, the complete removal of the wheel-axle assembly must take place, so a thorough inspection can be conducted. The disassembly and inspection do not afford the railcar owner the option to reuse any of the suspension elements, including the high-priced Guardian Bearing [22]. A recent review that provides a detailed summary of most of the onboard condition monitoring sensors, systems and techniques for freight railway vehicles can be found in reference [23]. One important takeaway from this review is the lack of reliable onboard load sensors that can accurately provide the load applied to each bearing on a railcar.

Most rail companies believe that bearing health monitoring is essential to the preservation of the industry. However, because of federal regulation, onboard condition monitoring systems remain in their infancy. The ideal system for bearing health monitoring would include vibration, temperature, and load sensing capabilities. Vibration monitoring can detect the onset of spall initiation and track its growth with service life. Temperature monitoring is perceived to detect impending catastrophic failure, whereas, load monitoring can help detect potential overloads or shifts in bearing loading, the effects of which, would only be evident in the vibration and temperature signatures at later times. Currently, most sensing units can measure temperature, and only a handful have the capability of measuring vibration. Two onboard load-sensing mechanisms are presently available to the industry. The first is patented by Union Tank Car Company and involves mounting load cells to the bottom of the rail car above the center bowl, enabling it to measure the load seen by four-bearing sets and not individual bearings [24]. The second is part of the asset monitoring initiative of AmstedRail™, which utilizes transducers and sensors to capture the weight of the railcar, but also does not specifically target bearing health [20]. By contrast, the load sensor-insert presented here provides an accurate and reliable onboard freight railcar load and temperature condition monitoring system that can be readily implemented with minor modifications to the current bearing-adapter assembly.

3 Design Specifications

The successful implementation of the Smart Adapter™ load-sensor insert depends on the strategic placement of the sensors within the adapter. For the most accurate measurements, the load sensor placement needs to be directly in the path of the applied load. The load is applied directly above the adapter's polymer steering pad, which sits on top of the railroad bearing positioned at the end of the wheelset. By placing the sensor directly between the polymer steering pad and the steel adapter, the sensor can then accurately detect the portion of the load seen by the bearing. Hence, one of the essential tasks of this study was the need to analyze the pressure distribution across the polymer steering pad, depicted by the blue component in Figure 3.

Figure 3: AdapterPlus™ - steering pad assembly

The design qualifications require that the sensor survive and monitor loads ranging from 26 kN (5.85 kips) to 153 kN (34.4 kips), which are the estimated unloaded (empty) and fully-loaded weights, respectively, of a class F and K railcar bearing (the total weight of a railcar can be calculated by multiplying these values by eight). Moreover, the sensor would need to transmit a reliable signal over the wide range of load unaffected by the impact forces that are generated by typical service operation, and by abnormal operation resulting from bearings with spalls and defects, impacts due to wheel flats, or bad segments of track.

The temperature sensors incorporated into the insert need to detect extreme bearing operating temperatures, *i.e.*, -40°C to 150°C (-40°F to 300°F). The temperatures around the circumference of the bearing vary. However, the highest temperatures are usually recorded at the region of load application, which is the area at the top of the bearing right under the steel adapter. To provide an accurate estimate of the highest temperature region of the bearing, the temperature sensors must be located at the top, right below the region of applied load, and near the centers of the inboard and outboard raceway portions of the bearing cup (outer ring).

4 Experiment and Terminology

4.1 Test Rigs

4.1.1 Single-bearing tester (SBT)

The Single-Bearing Test Rig, depicted in Figure 4, was used to carry out the series of experiments for constant load correlations. The test rig can closely mimic field service operation and can simulate numerous normal and abnormal load conditions a railroad bearing might experience in the field, making it favorable for laboratory-controlled experimental testing. The single-bearing test rig allows for both static and dynamic testing with speeds varying from 8 to 137 km/h (5 to 85 mph) under loads ranging from 10-120% of full-load; full-load being153 kN (34.4 kips) per bearing.

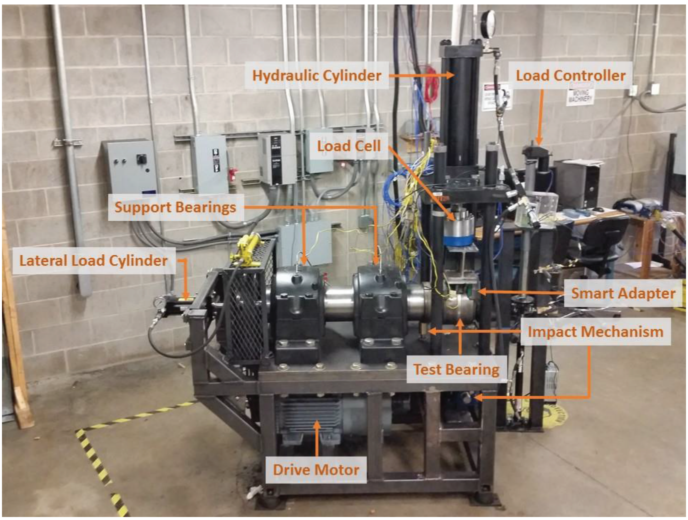

Figure 4: Single bearing tester (SBT)

4.1.2 Environmental chamber four-bearing tester

A four-bearing tester housed within an environmental chamber, shown in Figure 5, was also utilized to generate a supplementary ramping calibration at several operating temperatures. Figure 6 illustrates the loading setup for the four-bearing test axle. The four-bearing test rig has similar capabilities to those of the single bearing tester in terms of static and dynamic load application, but it provides the additional temperature parameter that is needed to validate the results acquired from the multivariate calibration. The environmental chamber is equipped with an industrial-strength air-conditioning unit and fans that control the ambient temperature, allowing the testing environment to range from -40˚C to 55˚C (-40˚F to 131˚F).

The motors used in both test rigs are 22 kW (30 hp) motors that are controlled using variable frequency drives (VFDs) that accurately maintain the desired angular speeds to within 0.5%. The VFDs can output the angular speed and the motor power simultaneously. The latter data is collected for every experiment to check for any abnormal operation during testing.

Figure 5: Four-bearing tester (4BT) housed in an environmental chamber

4.2 Load Controller

The test rigs used in all experiments utilize a hydraulic cylinder for load application. To counter the effects of thermal expansion of the oil within the hydraulic cylinders, an external load controller device was fabricated and used. The load controller apparatus is an additional, reactionary, 38 mm (1½-inch) bore hydraulic cylinder driven by a linear actuator, which transforms the rotational movement of a DC motor to translational movement through a threaded rod via a gearbox. A computer equipped with a DAQ (data acquisition) device and the software LabVIEW™ provides the ability to run extremely detailed testing plans.

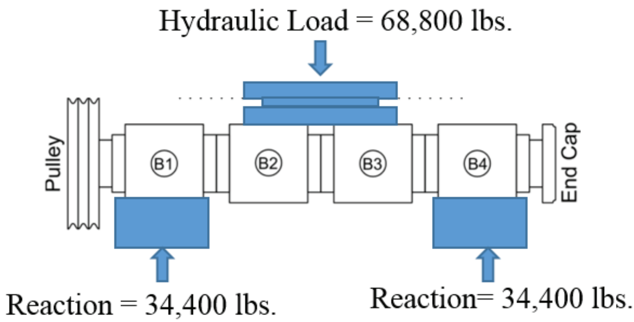

Figure 6: Load distribution on four-bearing tester

An error loop in the program reads the force defined by the load cell voltage. It then regulates the load the hydraulic cylinder applies and determines whether to increase or decrease the pressure. If the error exceeds a pre-programmed value, the analog output in the port of a NI USB-6211 DAQ sends a five-volt pulse signal to the motor controller until the force applied is within the specified tolerance.

The load controller can provide a steady, accurate load at a resolution of ±445 N (100 lb_f); however, when conducting dynamic testing, the impact forces generated by the rotation of the axle can fluctuate the load significantly, well above the ±445 N range. For the most part, these fluctuations are due to geometric raceway tolerances. Nonetheless, an error range of ±1,560 N (350 lb_f) was utilized for the experimental testing. The system can additionally execute programmed test plans that simulate loading cycles at varying rates for prolonged periods of time. Although, the device can function independent of human supervision, for simulation purposes, the axle rotation was physically stopped when loading or unloading the bearing to accurately mimic actual loading/unloading scenarios in field service.

4.3 Data Acquisition

For both test rigs, a computer with a National Instruments™ cDAQ-9474 USB chassis coupled with a NI 9205, 32 channel, ±10 Volt analog input module collected the data for the experiments at a sampling rate of 50 Hz. The information was then post-processed in MATLAB™ with a moving average of 200 data points corresponding to four seconds of averaged data. The decision for this specific averaging window is intentional. The averaging allowed for the alignment of the load sensor data with currently used accelerometers affixed to the two test rigs. In future testing, the load and temperature data acquired from the load sensor insert coupled with the vibration sensor data could provide a comprehensive onboard condition-monitoring technology.

4.4 Strain Gauge and Flex Circuit

The strain gauge used in the load sensor-insert is manufactured by Micro Measurements™. It is a full-bridge, transducer class device with a 350-Ohm nominal resistance. Four resistors make-up the full-bridge strain gauge. The device is adhered to a surface, and when the surface of the material strains, it alters the resistance of the circuit. The transducer holds two active resistors considered "axial" gauges. These resistors measure the strain experienced in the bending direction of the sensor. The remaining two eliminate changes that occur due to thermal expansion of the wiring. They are termed "temperature compensation" resistors or "transverse" gauges and are oriented with the neutral or non-bending axis of the sensor insert. Temperature compensation works by subtracting the voltage potential change due to temperature shifts in the transverse gauges from the output of the active gauges. Therefore, a full-bridge transducer strain gauge only detects changes caused by deformation.

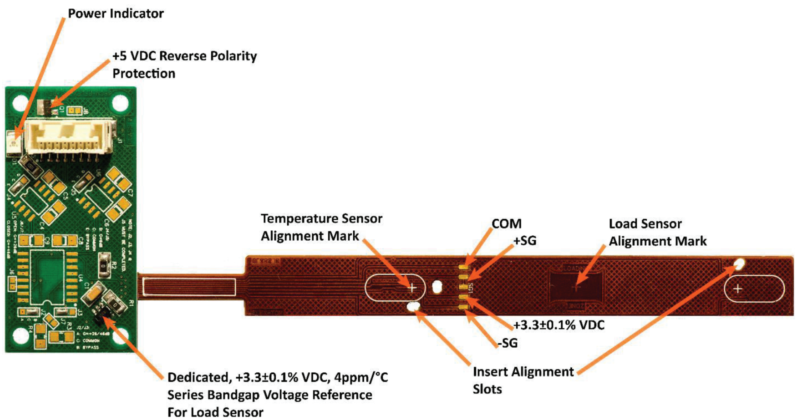

Figure 7: Adapter sensor insert flex circuit

Additionally, a specially designed flex circuit, shown in Figure 7, was utilized to provide wiring to the load insert. The insert design created numerous constraints that made the flex circuit a suitable choice improving functionality and reliability because of its ultra-thin design. The flexible sheet also provides a secure location for the two analog, surface-mount temperature sensors without the need for additional wires. Despite its thin appearance, the flex circuit requires some clearance to avoid both damage to the strain gauge and uncertainty in the results. If enough clearance is not provided, the sensor may display random errors in the measured load [16]. The load sensor insert assembly and the machined adapter that houses the load sensor insert are pictured in Figure 8 and Figure 9, respectively.

Figure 8: Load sensor insert assembly (top view)

Figure 9: Bearing adapter machined for load sensor insert compatibility

Finally, it is important to note that the effects of machining the bearing adapter to accept the load and temperature sensor insert on the structural integrity and fatigue life of this steel adapter have been thoroughly studied in previous published work by the UTCRS research group [25-26].

4.5 Load Signal Conditioning

All strain gauges must be signal-conditioned with an appropriate amplifier. Thus, the INA 129 instrumentation amplifier, produced by Texas Instruments™, was chosen because it is a low-power, high-accuracy device that features adjustable gain by means of a single resistor. Although the amplifier can reach a maximum gain of 600V/V, only a gain of 400V/V was utilized to attain an output range of three to ten volts. The signal was also conditioned using a MAX 294 8^{th} order chip, which is a low-pass filter designed by Maxim Integrated Products Inc.

Once the initial schematic of the load signal-conditioning circuitry was drafted, it was transferred to DipTrace™, a printed circuit-board design software. A schematic of the flex circuit was constructed and sent for production. The entire circuitry can simultaneously measure four strain gauges and eight temperature sensors for a total of four load-sensing insert devices.

4.6 Adapter Steering Pad

The AdapterPlus™ steering pad is an injection molded thermoplastic polyurethane (TPU) product produced by Steinmetz, Inc. [27]. The pad is an important part of the assembly because it prevents metal-to-metal contact, promotes more efficient steering, and can survive high-operating temperature conditions. The steering device is classified as a viscoelastic material and will exhibit creep under a constant load as well as relaxation when the weight is removed. Creep is the tendency of a material to flow, or deform, under an applied force. For this application, the elastomer pad is what allows the insert to deform under the weight of the railcar. Unfortunately, because the material flows away from the point of load application, it results in a change of pressure distribution over time.

Findley *et al.* [28] describes how the changes experienced by a viscoelastic material subjected to stress and strain are time and temperature-dependent. Since the elastomer polymer pad used in the AdapterPlus™ is a viscoelastic material, an accurate correlation relating strain gauge readings to load must also incorporate temperature and strain rates to account for the creep behavior. To further explain, although the full-transducer strain gauge compensates for thermal effects within its circuitry, the temperature-dependent creep of the polymer pad has a measurable effect on the sensor output. This thermal effect must be properly defined and incorporated into the system analysis.

Furthermore, before any calibration can be attained, the AdapterPlus™ steering pad must be allowed a settling time. It must creep under the weight of the railcar, simulated by the hydraulic cylinder. To this end, the test rigs are loaded up to the proportional full weight of a railcar and run at 40 km/h (25 mph) for at least 24 hours before testing. This process allows the elastomeric material of the steering pad to conform to its "loaded equilibrium" that lasts throughout the usage of the assembly.

4.7 Testing Overview

It is important to state that dynamic testing refers to experiments with active rolling elements, in other words, the test axle is rotating at a prescribed rotational speed during the experiment. Dynamic experiments mimic the service environment of a moving freight railcar with impact forces generated by the vibrations within the bearing assembly. Alternately, static testing lacks axle rotation.

The first experiment, plotted in Figure 10, was designed to devise a calibration for a fully-loaded railcar (34.4 kips or 153 kN per bearing) whilst maintaining accuracy during unloaded (empty railcar) conditions. The test was run at a laboratory temperature of 25°C on the single bearing test rig pictured in Figure 4. The experiment entailed three eighteen-hour loaded segments of dynamic testing separated by six-hour unloaded periods (5.85 kips or 26 kN per bearing). The latter was followed by static testing that consisted of several eight-hour constant load segments separated by one-hour unloaded periods, as shown in Figure 10.

During the dynamic testing, the test axle simulated a railcar traveling at a speed of 40 km/h (25 mph). Therefore, each eighteen-hour loaded interval (83%, 99%, or 100% of full-load) resulted in approximately 720 km (450 miles) of travel simulating a rail line distance starting, for example, in Houston, Texas traveling through San Antonio and stopping in Fort Worth, Texas. The 17% load (typical weight of an empty railcar) operation segments resulted in approximately 201 km (125 miles) of rail track traveled. Static testing conditions utilized load steps of 17%, 80%, and 100% of full-load. From the test overview shown in Figure 10, it can be observed that there are three loaded segments during the dynamic testing and four loaded intervals during the static testing.

The second set of experiments were carried out utilizing the four-bearing test rig, which is housed in the environmental chamber, and they incorporated temperature and ramping effects into an optimized calibration. Again, all testing was conducted after allowing for the 24 hour “settling time” described earlier. The system started with a loading of 52 kN (11.7 kips), which is equivalent to an unloaded railcar, and ramped up to 306 kN (68.8 kips), which is the load equivalent to a fully-loaded wagon. Note that these values are doubled since the hydraulic cylinder on the four-bearing test rig applies load on the two middle bearings simultaneously – see Figure 6. The experiments encompassed static ramping tests of 1.5, 2, 3, 5, and 7 minutes that were carried out at different ambient temperatures of -10, 0, 10, 20, 35, and 50˚C. Once full-load, as indicated by the load cell, was reached, the hydraulic system load controller maintained the load according to the sensor for approximately 120 seconds. Additionally, dynamic two-minute ramp experiments, at speeds of 53 and 106 km/h (33 and 66 mph), were performed at the various temperature conditions stated earlier.

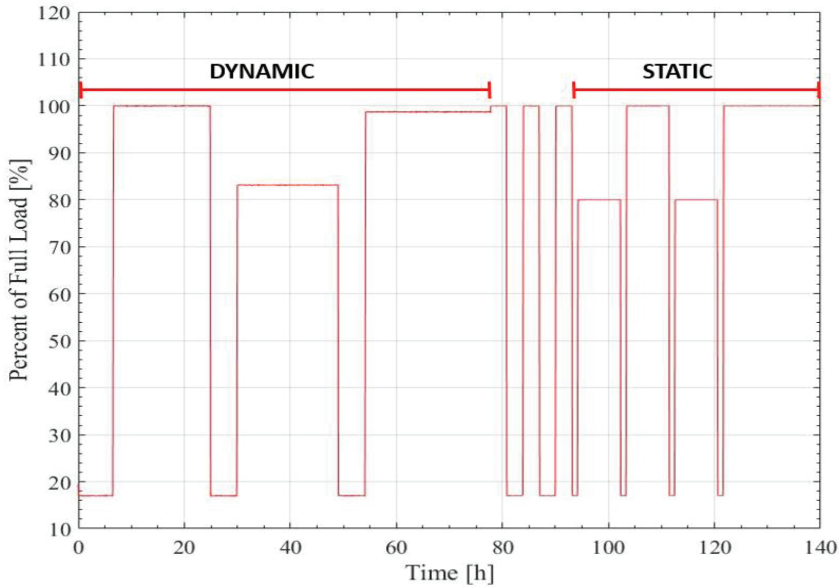

Figure 10: Typical test overview

5 Results and Discussion

To make the load sensor insert an integral part of any condition-monitoring system, a proper calibration must be integrated. Without accuracy and precision, the load sensor would lack proper functionality. The multivariate calibration provided the basis for a fully calibrated load sensor system. By evaluating constant load and ramping conditions, the final multivariate calibration was developed and validated.

5.1 Constant-Load Calibration

For the constant load calibration, two correlation methods were compared on the single bearing test rig. The first method was a second-order calibration with the scheme shown in Figure 11. The second method was a multivariate correlation, shown in Figure 12, which includes a regression algorithm that incorporates temperature information to define the relationship between the strain-gauge conditioned signal and the applied force as measured by the load cell (reference value). A multivariate correlation defines the relationship between the parameter data collected in an experiment to optimize the accuracy and precision of a certain prototype or device.

To devise both calibration methods, several iterations of known load conditions were run, after the allotted 24-hour "settling time". The voltage output from the signal conditioning box was measured. Once data were recorded both from the load cell and the signal conditioning box via the data acquisition system described in Section 4.3, a MATLAB™ script was run to correlate all the acquired information.

The full dynamic and static portions of testing were used to obtain the coefficients listed in Table 1. The second-order correlation utilizes three coefficients; namely, an offset, and two values related to the voltage output of the sensor with units of volts and square volts. In contrast, the multivariate correlation has six coefficients; namely, an offset, two voltage-dependent coefficients, two temperature-dependent coefficients, and one pairing of the two parameters.

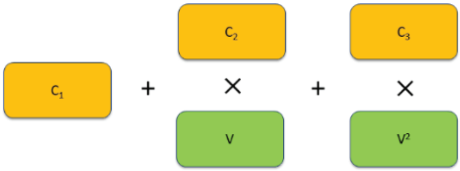

Figure 11: Second-order correlation scheme obtained utilizing the single bearing tester. [C = Constant Coefficients, V = Load-Sensor Voltage]

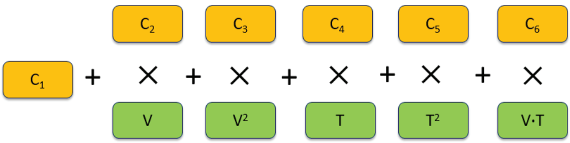

Figure 12: Multivariate correlation scheme obtained utilizing the single bearing tester. [C = Constant Coefficients, V = Load-Sensor Voltage, T = Temperature]

Second-Order Correlation		
C_1	C_2	C_3
$[V_0]$	$[V]$	$[V^2]$
-23490	7157	344

Table 1: Second-order correlation coefficients. [C1, C2, and C3 are constant coefficients and V is the load-sensor voltage]

Multivariate Correlation					
C_1	C_2	C_3	C_4	C_5	C_6
$[V_0]$	$[V]$	$[V^2]$	$[T]$	$[T^2]$	$[V \cdot T]$
-53972	15165	-197	856	-6	-123

Table 2: Multivariate correlation coefficients. [Cs are constant coefficients, V is the load-sensor voltage, and T is the temperature]

5.1.1 Empirical results – dynamic testing

In Figure 13, the dynamic portion of testing which employs the second-order correlation is presented. The data shows that this method slightly underestimates the load of the bearing with the axle rotating. The correlation had an overall error of 1.65% for the "loaded" portion of the testing, which corresponds to a difference of 2.53 kN (568 lb_f) between the load insert strain-gauge measurement and the load-cell reading (used as the reference). The test results applying the multivariate correlation can be seen in Figure 14. Utilizing multivariate regression analysis, the sensor load measurements match the load-cell readings more closely. The overall average error for the loaded portions of the dynamic test is 1.12%, which corresponds to a 1.71 kN (385 lb_f) error in the strain-gauge load measurement.

For both the second-order and the multivariate correlations, the sensor overestimates the actual load for a little over three hours at the initial 100% load step. It is speculated that this initial overestimation can be attributed to the loading rate of the system, which results in a high-pressure distribution in the region of the applied load. After several hours have passed, the test rig reaches its steady-state temperature, which allows the sensor accuracy to improve. The sudden load overshoot observed at the initial 100% load step does not occur in the successive loading steps, as can be seen in Figures 13 and 14.

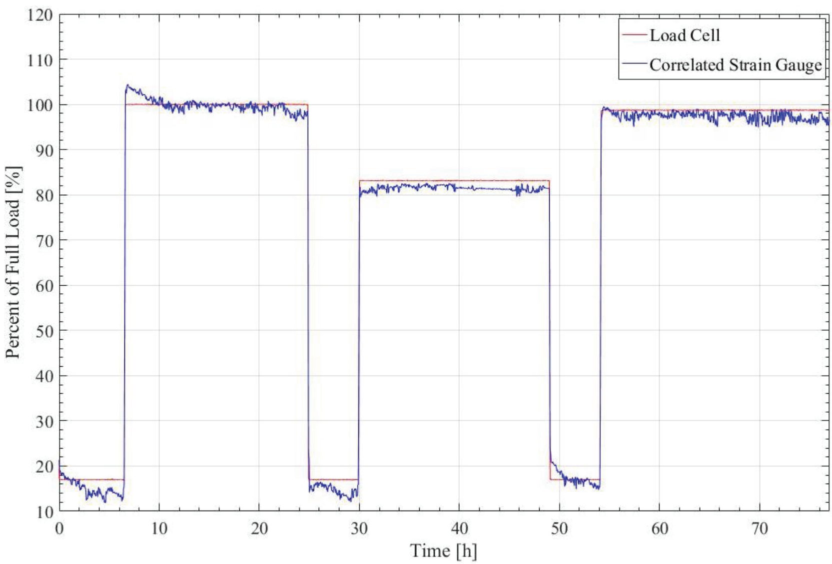

Figure 13: Dynamic test utilizing the second-order correlation

5.1.2 Empirical results – static testing

Unlike the dynamic testing results, the second-order calibration for static testing (bearing axle not rotating) tends to overestimate the load on the bearing-adapter assembly. However, the error, seen in Figure 15, is about 1% for the initial load step. The average error for the entirety of the static testing is around 1.41%, which corresponds to a 2.16 kN (485 lb$_f$) difference in load between the correlated sensor reading and the actual load value.

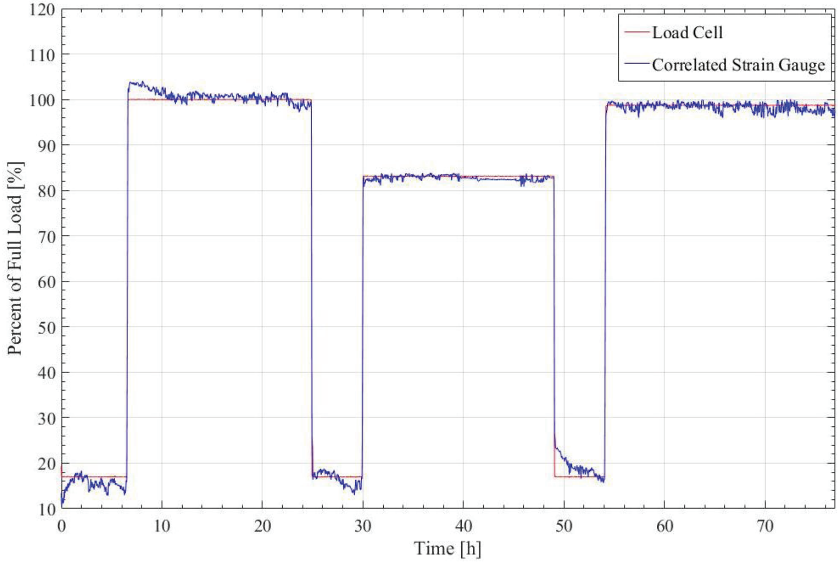

Figure 14: Dynamic test utilizing the multivariate correlation

The average error for the loaded portions of the static testing utilizing the multivariate correlation is merely 0.43%, which corresponds to only 658 N (148 lb$_f$) of freight. The results plotted in Figure 16 clearly demonstrate that this multivariate correlation more accurately reflects the load seen by the bearing and outperforms the second-order correlation by approximately 1.45% (2.22 kN or 499 lb$_f$) over the static testing period.

5.1.3 Discussion of constant load calibration results

When the bearing raceway temperature data was incorporated into the correlation to create the multivariate correlation, the accuracy of the load measurement improved considerably. The error throughout testing for the load sensor was 2.41% when using the second-order correlation. However, when the multivariate regression correlation was implemented, the error decreased to 1.56%, which corresponds to a load disparity of approximately 1,300 N (292 lb$_f$).

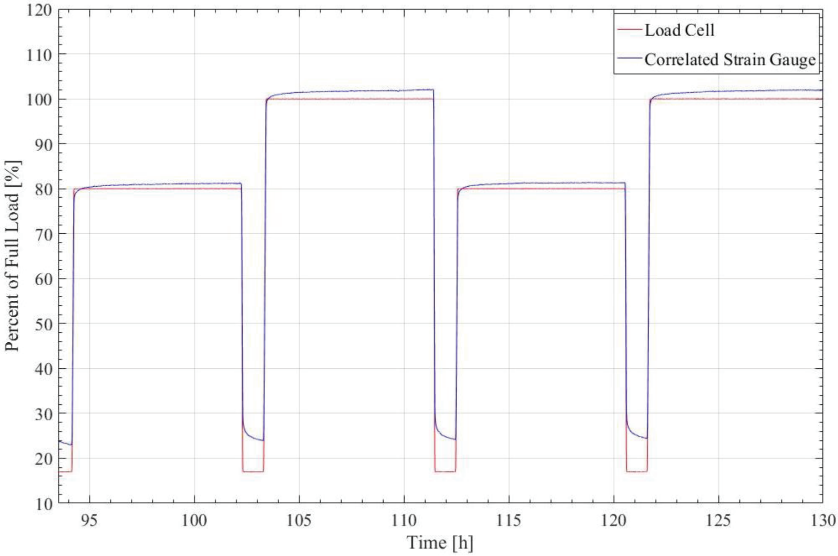

Figure 15: Static test utilizing the second-order correlation

Table 3 provides a summary of the results from the testing performed on the load sensor insert. The test parameters listed in the table define how the tests were categorized. The table also displays the calculated average errors corresponding to each portion of the experiment. The error was computed by taking the root-mean-square of the difference between the correlated load sensor readings and the actual load values taken by the load-cell and dividing that difference by the operating full-load of a class K bearing. Therefore, all percent-errors can be multiplied by 153 kN (34.4 kips) to determine the error value in Newtons or (pounds). The load difference (in Newtons and pounds) between the multivariate correlation and the second-order correlation is given in the rightmost column of Table 3. The results for all operating conditions verify that the multivariate correlation is more accurate than the second-order scheme proving that incorporating temperature conditions into the calibration significantly improves the accuracy of the load sensor insert measurements.

It should be noted that all the error calculations were carried out utilizing the load data that was collected five minutes after the load was applied. Any data prior to the five-minute marker is excluded from the error calculations. The latter was done due to the creep behavior of the elastomer pad that requires some settling time after an abrupt large load is applied. The load-sensor insert assembly voltage and temperature data are provided elsewhere [29].

Calculated Average Errors for Various Test Segments			
Test Parameters	Second-Order Correlation [%]	Multivariate Correlation [%]	Estimated Load Difference [N] / [lb_f]
All Testing Combined	2.41	1.56	1300 / 292
Dynamic – Fully Loaded	1.65	1.12	810 / 182
Static – Fully Loaded	1.41	0.43	1500 / 337
Dynamic – Unloaded	1.82	1.49	507 / 114
Static – Unloaded	3.11	1.66	2220 / 499

Table 3: Load sensor measurement optimization test summary

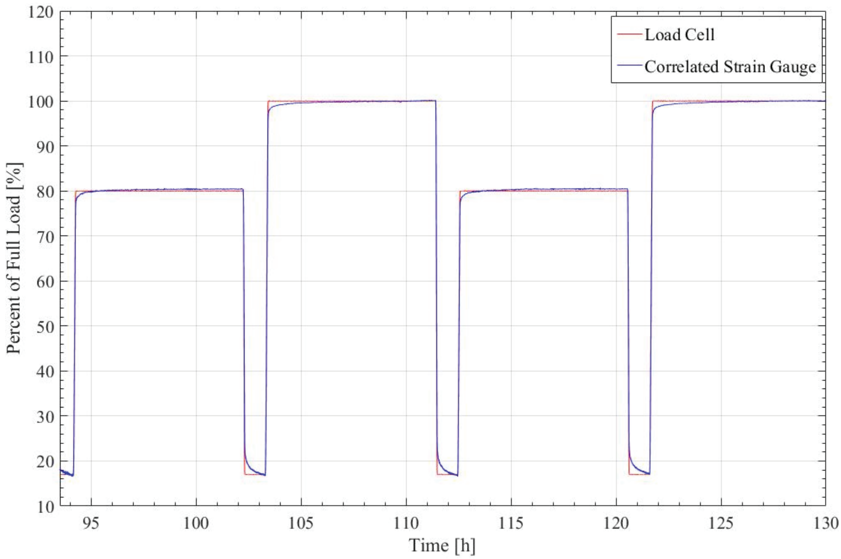

Figure 16: Static test utilizing the multivariate correlation

5.2 Optimized Calibration

Once it was established that the multivariate correlation was the optimal method for calibrating the load sensor insert, testing was carried out to develop an optimized algorithm that accurately represented the entire load ramping process without the need to ignore the five-minute settling period. In addition, the optimized calibration would account for the effects of ambient conditions. The test rig utilized for this optimized calibration correlation is the four-bearing tester which is housed in an environmental chamber (see Figure 5). As stated earlier, the test rig can operate under various ambient conditions allowing for data from two load sensor inserts (i.e., two strain-gauges and four temperature sensors) to be read and recorded simultaneously. The multivariate calibration was carried out following a similar scheme to that shown in Figure 12. Since more than one device was included, an additional sensor calibration was added to the algorithm, which resulted in more correlation coefficients, as seen in Figure 17 and Table 4. Note that the experiments performed to develop the optimized load sensor insert calibration utilized various load ramping rates as well as a few different operating temperature conditions.

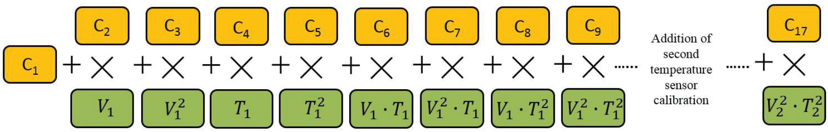

Figure 17: Optimized calibration scheme taking temperature and load ramping into account. [C = Constant Coefficients, V = Load-Sensor Voltage, T = Temperature]

Optimized Calibration								
C_1	C_2	C_3	C_4	C_5	C_6	C_7	C_8	C_9
	$[V_1]$	$[V_1^2]$	$[T_1]$	$[T_1^2]$	$[V_1 \cdot T_1]$	$[V_1^2 \cdot T_1]$	$[V_1 \cdot T_1^2]$	$[V_1^2 \cdot T_1^2]$
	17891	850	0	12	-63.6	-2	-28	0.861
$[V_0]$	C_{10}	C_{11}	C_{12}	C_{13}	C_{14}	C_{15}	C_{16}	C_{17}
	$[V_2]$	$[V_2^2]$	$[T_2]$	$[T_2^2]$	$[V_2 \cdot T_2]$	$[V_2^2 \cdot T_2]$	$[V_2 \cdot T_2^2]$	$[V_2^2 \cdot T_2^2]$
-4200	-24516	3046	-693	0	807	-10.3	-119	2.15

Table 4: Optimized calibration coefficients. [Cs are constant coefficients, V is the load-sensor voltage, and T is the temperature]

5.2.1 Optimized-Ramping Calibration Results

For most static tests at various ambient temperatures, the load sensor produced a steady signal for the different ramping rates. These experiments demonstrated that incorporating temperature into the calibration correlation along with the addition of more coefficients markedly reduced the percent error in loading. Results presented in Table 5 show less than 1% error in the load measurements for almost every full-load ramp at the various ambient temperatures. A maximum error of 1.63% was detected for the two-minute ramping test at 0°C, which corresponds to approximately 2.49 kN (560 lb_f) on a full-load scale. The various experiments performed can be displayed in graphs like the one shown in Figure 18, which represents a column from Table 5 – the ramp rate testing conducted at 20°C, whereas, Figure 19 captures the two-minute ramp time for the various ambient temperature conditions – a row on the average percent error table.

Ramp Rate [kN/min] / [kips/min]	Ramp Time [min]	Calculated Average Percent Error [%]					
		-10˚C	0˚C	10˚C	20˚C	35˚C	50˚C
102.0 / 22.9	1.5	0.09	0.37	0.17	0.18	0.21	0.15
76.5 / 17.2	2.0	0.88	1.63	0.69	0.22	0.18	0.29
51.0 / 11.5	3.0	0.27	0.57	0.33	0.19	0.20	0.12
30.6 / 6.9	5.0	0.17	0.59	0.58	0.14	0.34	0.09
21.9 / 4.9	7.0	0.19	0.35	0.05	0.17	0.54	0.11

Table 5: Average percent error for various ambient temperatures at full-load [load ramping occurs from 0 to 306 kN (68.8 kips) on two bearings (refer to Figure 6) over the listed time]

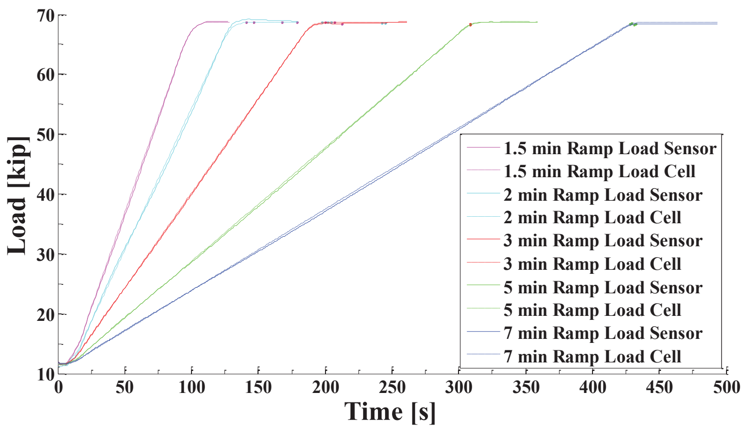

Figure 18: Multivariate correlation for the different ramping rates at 20˚C

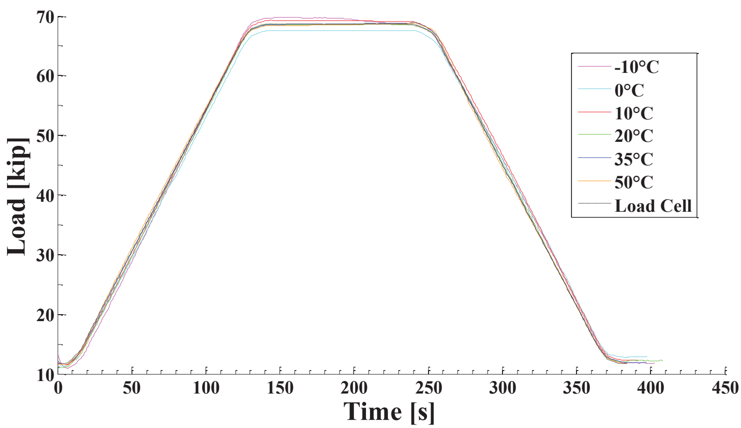

Figure 19: Multivariate correlation for the two-minute-static ramp test at various ambient conditions

Since the highest percent error occurred at the two-minute-static ramp rate test, the last set of experiments conducted were the two-minute-dynamic load ramps for a test rig with a rotating axle at speeds of 53 km/h (33 mph) and 106 km/h (66 mph) for various ambient temperatures. The results listed in Table 6 indicate that a maximum average error of 2.16% occurred at 106 km/h (66 mph) for an ambient temperature of 35˚C, which corresponds to a load of approximately 3.29 kN (740 lb_f). The latter load error is the result of the dynamic impacts of the rotating bearing elements that affect the load sensor readings. The sensor calibration is provided in Figure 20 for the 53 km/h (33 mph) speed; and in Figure 21 for the 106 km/h (66 mph) speed. Note that, freight cars are usually loaded statically or at very low speeds (10 km/h or 6 mph), so the average percent error data presented here for the dynamic load ramp tests represents a worst-case scenario to demonstrate the accuracy and repeatability of the developed load sensor under different operating conditions.

Ambient Temperature [˚C]	Average Percent (%) Error at 53 km/h (33 mph)	Average Percent (%) Error at 106 km/h (66 mph)
-5	0.85	0.61
5	0.37	0.61
15	0.64	0.96
25	0.97	0.73
35	1.25	2.16
50	0.37	0.78

Table 6: Dynamic average percent errors for various ambient temperatures

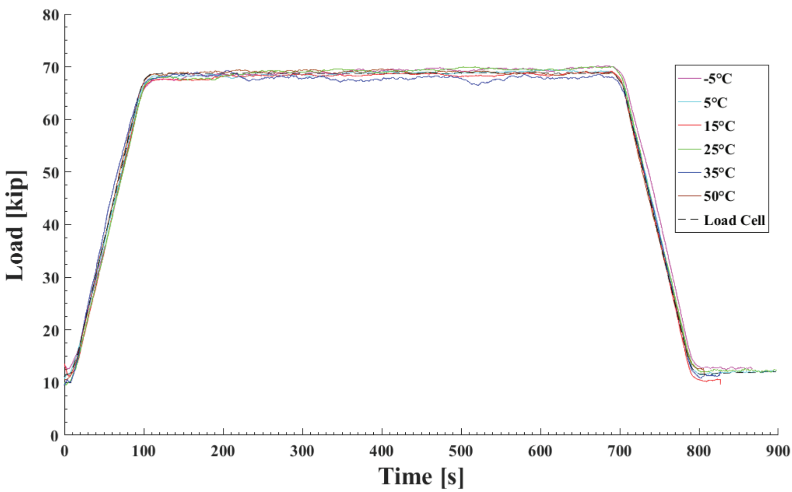

Figure 20: Multivariate correlation for the two-minute-dynamic ramp test for a speed of 53 km/h (33 mph) at various ambient temperatures

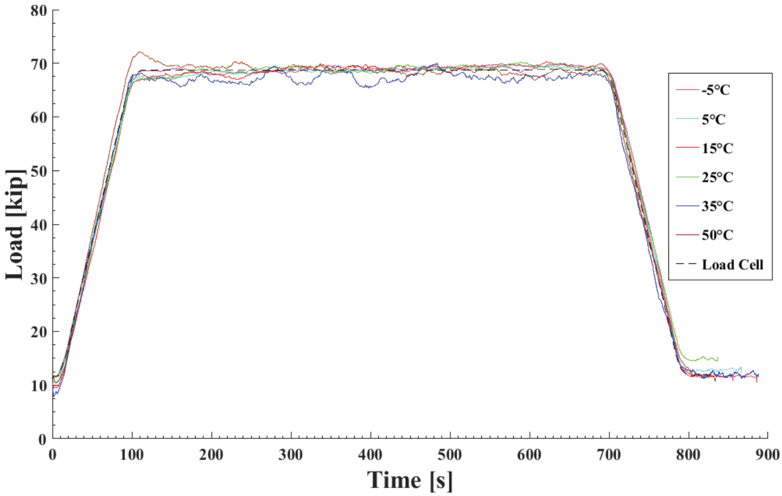

Figure 21: Multivariate correlation for the two-minute-dynamic ramp test for a speed of 106 km/h (66 mph) at various ambient temperatures

6 Conclusion and Future Work

Currently, the railroad industry utilizes weighbridges at special sections of track to measure the load of freight cars. These weighbridges are found in railyards and freight loading stations and are not commonly present along the 140,000 rail miles operated by the U.S.A. railroad companies. Thus, once the freight car leaves the railyard, it is not possible for the operator to continuously track the railcar load, which is especially important for railcars carrying hazardous material.

To this end, an onboard load sensor that can accurately and reliably track the load was developed and validated in the laboratory through carefully designed experiments that mimic field service conditions. The load sensor is strain-gage-based and is encapsulated within a steel insert that sits just below the polymer steering pad on a groove on top of the bearing steel adapter. Eight of these load sensor inserts are used on one freight car to determine the total weight of the railcar. Furthermore, each load sensor insert is equipped with two temperature sensors that measure the bearing operating temperature at both outer ring (cup) raceways. Hence, other than accurately tracking the weight of a railcar, the load sensor insert is also capable of identifying any abnormal operation conditions caused by load shifting within the freight car or unusual bearing operating temperatures.

The paper presented here provides detailed information on the design criteria and specifications of the load sensor along with all the laboratory testing performed to validate the design functionality and proof of concept. Two methods of calibration were examined: one second-order method and one multivariate regression method.

Several testing scenarios were carried out which produced repeatable and optimized results. The incorporation of raceway temperatures into the calibration algorithm of the load sensor insert allows for improved accuracy in the estimation of the load applied on the bearing adapter. The average percent error in the load readings for a stationary or moving fully-loaded railcar was within 1%, which is remarkable considering the nonlinear creep behavior of the polymer steering pads.

Even though the prototype load-sensor insert assembly has undergone short-duration proof of concept and validation field-testing performed at the Transportation Technology Center Inc. (TTCI) in Pueblo, Colorado, this technology needs to undergo long-term field-testing in rail service to ensure that the simulations conducted in the laboratory setting are applicable to field implementation. Similar to the short-duration field-testing conducted at TTCI, the long-term field test would incorporate eight load sensor insert assemblies and focus on the 17% (empty railcar) and 100% (full railcar) load scenarios to provide data that can be compared to the laboratory results; thus, demonstrating to the railroad industry that the load sensor can be successfully implemented in freight service. Note that the wireless battery-powered version of the prototype load-sensor insert, currently under development at the UTCRS, would be more suitable for the proposed long-term field-testing in rail service. Even though these load sensor inserts have been used to perform numerous laboratory and field experiments over the past five years, service lifetime testing might also be needed to quantify the durability of these devices in field service.

Finally, it is believed that the incorporation of accelerometers to the current load sensor insert that encompasses load and temperature sensors will expand the usage of this device as a complete bearing condition monitoring system that can detect the onset of failure at an early stage. The latter can be very important in developing proactive maintenance schedules that can greatly reduce unnecessary and costly train stoppages and delays.

Acknowledgments

The authors wish to acknowledge the financial support from the University Transportation Center for Railway Safety (UTCRS) which is funded through USDOT Grant No. DTRT13-G-UTC59. The authors also wish to thank Amsted Rail Industries, Inc. and their engineers for their help and assistance.

References

[1] "Freight Rail Today." Federal Railroad Administration. [Online]. Available: www.fra.dot.gov/Page/P0362. [Accessed 6 June 2016].

[2] D. Heyman and R. Perez-Pena, “Spilled Oil Keeps Flames Burning After a Train Derailment in West Virginia,” New York Times. 17 February, 2015. [Online]. Available: www.nytimes.com/2015/02/18/us/west-virginia-train-derailment-dumps-oil-into-river.html?_r=0. [Accessed 17 November 2016].

[3] J. Ley, “Load Sensor in an Elastomer Suspension Element,” Master’s Thesis, University of Texas-Pan American, Edinburg, TX, United States. 2012. Print.

[4] "Double Row Tapered Roller Bearings." SKF Bearings. [Online]. Available: www.skf.com/us/products/bearings-units-housings/roller-bearings/tapered-roller-bearings/double-row-tapered-roller-bearings/index.html. [Accessed 26 July 2016].
[5] C. Tarawneh, J. Aranda, V. Hernandez, and C. Ramirez, “An Analysis of the Efficacy of Wayside Hot-Box Detector Data,” Proceedings of the 2018 ASME Joint Rail Conference, Pittsburgh, PA, April 18-20, 2018.
[6] A. Mealer, C. Tarawneh, and S. W. Crown, “Radiative Heat Transfer Analysis of Railroad Bearings for Wayside Hot-Box Detector Optimization,” Proceedings of the 2017 ASME Joint Rail Conference, Philadelphia, PA, April 4-7, 2017.
[7] "Tapered Roller Bearing Units TAROL Products and Services." Schaeffler. [Online]. Available:www.schaeffler.com/remotemedien/media/_shared_media/08_media_library/01_publications/schaeffler_2/tpi/downloads_8/tpi_155_de_en.pdf, [Accessed 12 December 2016].
[8] "Tapered Roller Bearings Information." Engineering360. [Online]. Available: www.globalspec.com/learnmore/mechanical_components/bearings_bushings/tapered_roller_bearings. [Accessed 4 September 2016]
[9] "NEM Solutions - Hot Axle and Box Detection -HABD: System for Measuring the Temperature of Rolling Stock Gearboxes, Disc Brakes and Wheels." NEM Solutions. [Online]. Available: www.nemsolutions.com/rail/hot-axle-and-box-detection/. [Accessed 12 August 2016].
[10] C. Tarawneh, B. M. Wilson, K. D. Cole, A. A. Fuentes, and J. M. Cardenas, “Dynamic Bearing Testing Aimed at Identifying the Root Cause of Warm Bearing Temperature Trending,” Proceedings of the 2008 ASME RTD Fall Technical Conference, RTDF2008-74036, Chicago, IL, September 24-26, 2008.
[11] C. Tarawneh, J. A. Kypuros, B. M. Wilson, T. W. Snyder, B. Gonzalez, and A. A. Fuentes, “A Collaborative On-Track Field Test Conducted to Verify the Laboratory Findings on Bearing Temperature Trending,” Proceedings of the 2009 ASME Joint Rail Conference, JRC2009-63056, Pueblo, CO, March 3-5, 2009.
[12] "Wayside Advanced Technology Systems (WATS)," Federal Railroad Administration. [Online]. Available: www.fra.dot.gov/Page/P0806. [Accessed: 12 August 2016].
[13] S. Karunakaran, "Bearing Temperature Performance in Freight Cars," ASME RTD Fall Technical Conference, Chicago, IL, September 11-12, 2007.
[14] J. A. Kypuros, C. M. Tarawneh, A. Zagouris, S. Woods, B. M. Wilson, and A. Martin, “Implementation of Wireless Temperature Sensors for Continuous Condition Monitoring of Railroad Bearings,” ASME RTD Fall Technical Conference, Minneapolis, MN, September 21-22, 2011.
[15] N. G. Nenov, E. M. Dimitrov and G. S. Mihov, "Sensor for Measuring Load on Wheels of Running Railway Vehicle," 28th International Spring Seminar on Electronics Technology: Meeting the Challenges of Electronics Technology Progress, 2005.

[16] T. Diedrich, “Onboard Load Sensor Prototype for Use in Freight Railcar Service,” Master’s Thesis, University of Texas-Pan American, Edinburg, TX, United States. 2015. Print

[17] K. N. Malakhov and N. Korotkov, "Certain Problems of Weighing Technique in Railroad Transport," Measurements of Mass. Available: www.documentslide.com/documents/certain-problems-of-weighing-technique-in-railroad-transport.html. [Accessed: 17 August 2016].

[18] “Weighing Terminals Brochure,” Mettler Toledo. Columbus, Ohio, United States, p. 2-6. 2015.

[19] J. G. Tabbachi, R. R. Newman, R. C. Leedham, D. A. Purta, G. G. Madered and R. Galli, "Hot Bearing Detection with the SMART-BOLT," Proceedings of the 1990 ASME/IEEE Joint Railroad Conference, p. 105-10, 1990.

[20] "IONX Asset Monitoring." Amsted Rail. [Online]. Available: www.amstedrail.com/products-services/ionx-asset-monitoring. [Accessed 6 June 2016].

[21] "Guardian Bearing (Sensor)." Timken. [Online]. Available: www.timkenbearings.com/pt-br/solutions/rail/products/Pages/GuardianBearing.aspx. [Accessed 14 June 2016].

[22] M. L. French, K. M. Iftekharrudin, D. R. Leeper, R. P. Samy and W. Hwang, “Bearing with Wireless Self-powered Sensor Unit,” The Timken Company, assignee, Patent US 6535135 B1, 18 March 2003.

[23] E. Bernal, M. Spiryagin, and C. Cole, “Onboard Condition Monitoring Sensors, Systems and Techniques for Freight Railway Vehicles: A Review,” IEEE Sensors Journal, 19 (1), pp. 4—24, 2019.

[24] R. S. Toms, “Electronic Weighing System and Method for Railcars,” Union Tank Car Company, assignee, Patent WO 2010093895 A1, 19 August 2010.

[25] J. Montalvo, A. Trevino, A. A. Fuentes, and C. Tarawneh, “Structural Integrity of Conventional and Modified Railroad Bearing Adapters for Onboard Monitoring,” Proceedings of the 2014 ASME IMECE Conference, Montreal, Canada, November 14-20, 2014.

[26] A. Trevino, A. A. Fuentes, C. Tarawneh, and J. Montalvo, “Fatigue Life Estimation of Modified Railroad Bearing Adapters for Onboard Monitoring Applications,” Proceedings of the 2015 ASME Joint Rail Conference, San Jose, CA, March 23-26, 2015.

[27] “Adapter Plus Steering Pad System,” Amsted Rail. [Online]. Available: www.amstedrail.com/products-services/adapter-plus-steering-pad-system. [Accessed 21 July 2016].

[28] W. N. Findley, J. S. Lai and K. Onaran, “Creep and Relaxation of Nonlinear Viscoelastic Materials,” New York Dover Publications. 1976.

[29] D. Blackwell, “Multivariate Calibration of a Load Sensor for Dynamic and Static Freight Railcar Applications,” Master’s Thesis, University of Texas Rio Grande Valley, Edinburg, TX, United States. 2016. Print